

Magnetic properties of $A_2Cu_nX_{2n+2}^{2-}$ systems

ROGER WILLETT,* TODD GRIGEREIT, KRIS HALVORSON
and BRIAN SCOTT

Department of Chemistry, Washington State University, Pullman WA 99164-4630, USA

Abstract. The magnetic behavior of planar bridged copper(II) halide dimers, trimers, and tetramers are summarized. The planar oligomers exhibit antiferromagnetic coupling. Dimeric $Cu_2X_6^{2-}$ ions can undergo one of two types of distortions: a tetrahedral twist distortion and a bifold, or scdia, distortion. Both distortions cause the exchange interaction to become ferromagnetic. Trimeric species have a $S = \frac{1}{2}$ ground state. Evidence for non-Boltzman depopulation of the excited quartet state is observed and is tentatively assumed to arise from frustrated intertrimer interactions. Comparison of the $X = Cl$ and $X = Br$ salts show that the antiferromagnetic contribution to the exchange coupling is approximately twice as large for the bromide salts as for the chloride salts. It is also seen that the coupling becomes more antiferromagnetic as the length of the oligomer increases.

Keywords. Copper(II) halide oligomers; magneto-structural correlations.

1. Introduction

Copper(II) halide salts have provided a particularly fruitful field for studying magneto-structural correlations. The flexibility of the copper(II) coordination sphere, coupled with the non-stereospecificity and bridging ability of halide ions, has provided a wide plethora of structures which can be explored (Smith 1976). The d^9 electronic structure of the Cu(II) ion leads to the occupancy of a single magnetic orbital on each metal site and a nearly isotropic (Heisenberg) magnetic exchange coupling. This makes both the analysis of the magnetic data and the theoretical interpretation of the magneto-structural correlations particularly straightforward. It has been shown by Hay *et al* (1978) that the exchange energy, $2J$, for the interaction of two spin $\frac{1}{2}$ ions, can be expressed by the combination of two terms,

$$2J = 2K_{ab} - 2(\epsilon_1 - \epsilon_2)^2/(J_{aa} - J_{bb}) = 2J_F - 2J_{AF}, \quad (1)$$

where the exchange and coulomb integrals, $K_{ab} > 0$, $J_{aa} > J_{bb}$, are slowly varying functions of the molecular parameters while ϵ_1 and ϵ_2 are the energies of the molecular orbitals formed from the magnetic orbitals on the two metal ions. The first term gives a ferromagnetic (FM) contribution; the second an antiferromagnetic (AFM) contribution. Semiempirical techniques (Hay *et al* 1978; Bencini and Gatteschi 1978) have been used to calculate ϵ_1 and ϵ_2 as a function of various molecular parameters. Hence, it is possible to predict qualitatively the effect that a particular change in molecular geometry will have on the strength of the exchange

*To whom all correspondence should be addressed.

coupling. This assumption that K_{ab} can be regarded as independent of geometry has been challenged (Kahn and Charlot 1980).

Experimentally, the foundation of magneto-structural correlation in dimeric systems is based on the results found in copper(II) hydroxide complexes (Hatfield 1985). Considering a planar $\text{Cu}_2\text{X}_2\text{L}_4$ system, it has been demonstrated experimentally that the exchange coupling changes linearly with J with the coupling being FM for angles less than 97.5° , where ϕ is the Cu-L-Cu bridging angle (Hatfield 1985). Calculations (Hay *et al* 1978; Bencini and Gatteschi 1980) show that $\epsilon_1 - \epsilon_2$ varies strongly with angle, with $\epsilon_1 - \epsilon_2 = 0$ at an angle near 90° .

The concept of orthogonality leading to FM interactions shows up more explicitly in the formulation of Kahn and Briat (1976). The exchange constant is written as

$$J = J_F + J_{AF}, \quad (2)$$

where

$$J_F = \frac{1}{2} m^2 \sum J_{\mu\mu}, \quad (2a)$$

and

$$J_{AF} = \frac{1}{2} m^2 \sum \Delta_\mu S_{\mu\mu}, \quad (2b)$$

with $\Delta_\mu = \epsilon_1 - \epsilon_2$ and $S_{\mu\mu}$ is the overlap integral of the two equivalent magnetic orbitals on the two metal atoms. Thus, in this formalism, the AFM contribution clearly disappears when the orbitals are orthogonal.

In this paper, we will discuss the magnetic behavior of symmetrically bridged $\text{Cu}_n\text{X}_{2n-2}^{2-}$ anions ($\text{X} = \text{Cl}^-$ or Br^-), both summarizing published data and presenting a number of new, exciting results. The structural properties of $\text{Cu}_2\text{Cl}_6^{2-}$ dimers have been discussed as part of a review of the structural characteristics of ACuCl_3 salts (Willett and Geiser 1984) while a summary of known pseudo-planar $\text{Cu}_n\text{X}_{2n-2}^{2-}$ anions has recently appeared (Geiser *et al* 1986). The magneto-structural correlations in bridged copper(II) halides were summarized some time ago (Willett 1985) but numerous other results have been obtained since that time, particularly for the $\text{Cu}_n\text{X}_{2n-2}^{2-}$ systems with $n = 3$ and 4, as well as for $\text{Cu}_2\text{Br}_6^{2-}$ dimers.

2. Magnetic behavior of $\text{Cu}_2\text{X}_6^{2-}$ dimers

2.1 Structural properties

Starting with the planar $\text{Cu}_2\text{X}_6^{2-}$ dimer (figure 1a), two possible distortions have been observed (Geiser and Willett 1984). One involves a twisted dimer (figure 1b) in which the copper(II) ion distorts towards a tetrahedral coordination geometry. The distortion is characterized by a twist angle, τ , between the bridging Cu_2X_2 plane and the terminal CuX_2 planes. The second involves a bifolded or "sedia" distortion, in which two terminal halide ions (one on each end of the dimer) are twisted out of the bridging plane. This distortion is characterized by a bifold angle, σ , between the central Cu_2X_2 plane and the terminal CuX_3 planes. Of interest

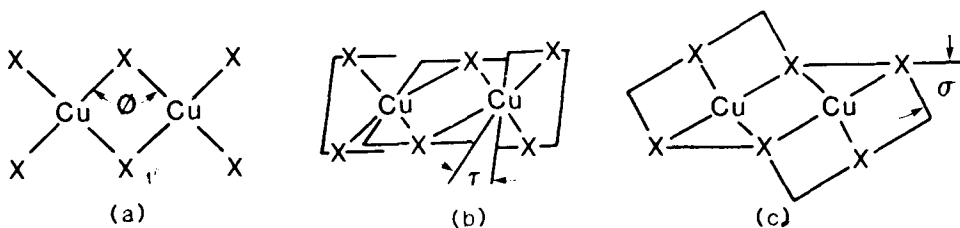


Figure 1. Distortions of the $Cu_2X_6^{2-}$ dimeric species. a) Planar; b) twisted; c) bifold or sedia.

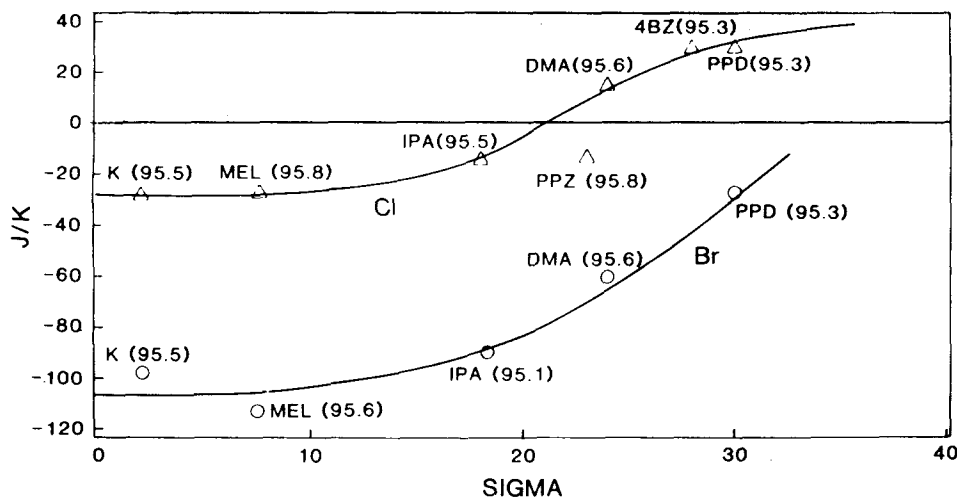


Figure 2. Plot of J/k vs bifold angle, σ , in $Cu_2Cl_6^{2-}$ and $Cu_2Br_6^{2-}$ dimers. (K = potassium, MEL = melaminium, IPA = isopropylammonium, DMA = dimethylammonium, PPZ = piperazinium, 4BZ = 4-benzylpiperidinium, PPD = piperidinium.)

magnetically, is the bridging Cu-X-Cu angle, ϕ . Thus, in discussing the magnetic properties of $Cu_2X_6^{2-}$ dimers, we are examining an exchange coupling hypersurface, which can be expressed as $J(\phi, \tau, \sigma, \dots)$. Among the other parameters affecting this complex surface will be the Cu-X distances, both within and between oligomers. Experimentally, it is desirable to study a series of systems where one, or at the most two, of these parameters vary.

The twisted dimers, with τ values typically in the range 40–50°, occur in structures where the dimers are structurally and magnetically isolated. The planar and sedia dimers generally occur in compounds where the dimers aggregate in stacks through the formation of 1 (sedia) or 2 (planar) semicoordinate Cu-X bonds per copper(II) ion between dimers. Two isolated planar dimers have been discovered in the last year (Honda *et al* 1985; Pellacani *et al* 1986). The range of the sedia distortion is substantial, going from $\sigma \sim 0$ out to $\sigma \sim 40^\circ$, with a large number of examples. In the sedia distortion, the *interdimer* Cu...Cl distance generally shortens as σ increases. Thus, in the limit or large σ , the copper(II)

coordination geometry approaches the trigonal bipyramidal limit. In the twisted dimers, $\phi \sim 93^\circ$, while in a majority of the planar or sedita dimers, $\phi \sim 95.5^\circ$ – 96.0° .

Calculations have been carried out by Hay *et al* (1978) as well as Bencini and Gatteschi (1978) for a series of distortions of dimeric species. Results of these calculations show, for example, that $|\epsilon_1 - \epsilon_2|$ increases as the bridging Cu–L–Cu angle, ϕ , increases when $\phi > 90^\circ$, in accord with the experimental observation of increasing antiferromagnetic character as ϕ is increased. For the twisted dimer, they also show that $\epsilon_1 = \epsilon_2$ at an intermediate value of the twist angle, τ . Thus, as τ increases from $\tau = 0$, the interaction is first predicted to become more ferromagnetic, reach a maximum value, and then decrease as $\tau \rightarrow 90^\circ$.

The dependence of exchange coupling on these distortions can be readily understood following simple orthogonality arguments. For the planar dimers, each localized unpaired electron lies in a $d_{x^2-y^2}$ -like antibonding molecular orbital. The unpaired electron density is substantially delocalized out into the P_σ orbitals on the ligands, with only a small contribution into the ligand Δ orbitals. Thus, for $\phi \sim 90^\circ$ the orbitals on the two copper centers will be nearly orthogonal, and a ferromagnetic interaction is anticipated from Hund's rule arguments. As ϕ increases, the overlap increases, giving an antiferromagnetic contribution to the exchange coupling. As the dimers distort from planarity, the lobes of the local metal orbitals no longer point directly at the ligands, so the contribution of the ligand orbitals in the magnetic orbitals is expected to decrease. Thus, there is less overlap of the two localized magnetic orbitals, decreasing the antiferromagnetic contribution. Hence, the coupling becomes more ferromagnetic, at least initially, as the distortion increases.

The magnetic susceptibility data for isolated dimers can be analyzed with a simple Heisenberg dimer model, perhaps including a mean field correction to account for weak interdimer contacts (Chow *et al* 1975). These are likely to be more important in bromide salts, due to its increased van der Waal's radius as compared to the chloride salts. The sedita dimers constitute alternating magnetic chains, with an intradimer exchange pathway, J , and an interdimer exchange pathway, J' . For J and $J' < 0$, expressions for $\chi(J, J')$ are available (Hall *et al* 1981). The value of $|J'|$ is generally smaller than the magnitude of $|J|$, since the semi-coordinate bonds are approximately perpendicular to the magnetic orbital and the differential overlap between magnetic orbitals on different dimers is quite small. Thus, the mean field dimer model can be used when one or both of J and J' are ferromagnetic. However, in the crossover region, where J changes from ferromagnetic to antiferromagnetic, $|J|$ and $|J'|$ can be of the same order of magnitude, which confuses the magnetostructural conclusion. This crossover region covers a relatively large range of σ values for the chloride salts, but is much smaller for the bromide salts. This makes the study of copper(II) bromides more rewarding. No model exists for the susceptibility of stacked, planar dimers, since three J' pathways exist between dimers. Fortunately, $|J'|$ is generally smaller than $|J|$ in these systems, so a mean field dimer model is usually appropriate. In addition, with $J < 0$, if all J' pathways have the same sign, spin frustration occurs, tending to cancel out effects of the interdimer interactions (see discussion of trimers). In any case, when $J < 0$, J is uniquely determined by T_{\max} , the temperature at which χ_m reaches a maximum with T_{\max} in the range $1.20 J/k - 1.25 J/k$.

2.2 Twisted dimers

The structural and magnetic data for systems containing isolated, twisted dimers are summarized in table 1. In addition to the ferromagnetic $(\phi_4A)CuX_3$ salts ($A = P, As, Sb$) (Bencini *et al* 1985), the planar dimers in the (morpholinium) CuX_3 salts (Scott and Willett 1987) are included, as is the infinite $(CuBr_2)_n$ chain of tetrahedra in $[(C_2H_5)_2NH_2]_2Cu_4Br_{10} \cdot EtOH$ (Fletcher *et al* 1983). The morpholinium salts have oxygen atoms from the morpholinium ions forming weak semi-coordinate bonds to the copper(II) ions, thus the dimers approximate isolated ions. From table 1, it is seen that as the coordination sphere twists towards tetrahedral, the bridging angle, ϕ , decreases substantially. The exchange coupling is antiferromagnetic for $\tau = 0^\circ$, becomes ferromagnetic for $\tau \sim 50^\circ$, and becomes antiferromagnetic again for $\tau \sim 85^\circ$. The initial decrease in the antiferromagnetic contribution to the exchange is readily understood, since the sedita distortion will cause the magnetic orbitals to twist out of the bridging Cu_2Cl_2 plane, thus leading to a decrease in the overlap of the magnetic orbitals at the bridging halides. Calculations for the twisted dimer, assuming $\phi = \text{constant}$, showed that $\epsilon_1 = \epsilon_2$ at $\tau \sim 30^\circ$ (Hay *et al* 1978). Thus, a maximum ferromagnetic interaction is expected at that point, with the coupling becoming more antiferromagnetic as τ changes from that value. The experimental data certainly confirm that general behavior. Extended Huckel calculations performed in our laboratory for the actual geometries of the $\phi_4AsCuCl_3$ and ϕ_4PCuCl_3 salts indicate that the maximum ferromagnetic value is expected at an τ angle slightly larger than 50° . Further experimental examples at different τ values are needed to fill out this section of the exchange energy surface.

2.3 Sedita dimers

A substantial series of stacked $Cu_2X_6^{2-}$ dimers have been synthesized and studied (O'Brien *et al* 1986; Willett 1986; Scott and Willett 1986) in conjunction with Prof. G. C. Pellacani's laboratory in Modena, Italy. These are listed in table 2, where it is seen that a fairly densely packed $J(\phi, \sigma)$ surface exists with $\sigma \leq 40^\circ$ and $95^\circ < \phi < 98^\circ$. In general, for $\phi \sim 95.5^\circ$, J is antiferromagnetic for small values of σ and becomes ferromagnetic for $\sigma > 25^\circ$. These data are plotted in figure 2 for both the chloride and bromide salts. The general trend from the data is clear, although considerable scatter is seen. This presumably is due to small changes in

Table 1. Structural and magnetic parameters for twisted $Cu_2X_4^{2-}$ dimers.

	ϕ	τ	J/k
(Morpholinium) $CuCl_3$	95.8	0	43
$(\phi_4As)CuCl_3^a$	93.8 ^c	48.2	28
$(\phi_4P)CuCl_3^a$	93.2 ^c	50.0	55
$(\phi_4Sb)CuCl_3^a$	94.6	44.4	65
(Morpholinium) $CuBr_3$	—	0	120
$(\phi_4As)CuBr_3^a$	—	-50	28
$(\phi_4P)CuBr_3^a$	—	-50	37
$[(C_2H_5)_2NH_2]_2[Cu_4Br_{10} \cdot EtOH]^b$	84.3 ^c	84.9	-21

^a Chow *et al* 1975; ^b See Willett and Geiser 1984 and references therein;^c Pellacani *et al* 1986.

Table 2. Structural and magnetic parameters of stacked planar or sedia $\text{Cu}_2\text{X}_6^{2-}$ dimers^a.

Cation	X = Cl					X = Br			
	ϕ (°)	Cu-Cl, bridging (Å)	σ (°)	J/k (K)	$\epsilon_s - \epsilon_a$ (eV)	ϕ (°)	Cu-Br, bridging (Å)	σ (°)	J/k (K)
K^+	95.5°	2.318	1.5°	-28	0.1153	—	—	—	-95
2-amino-3-hydroxy- pyridinium ⁺	—	—	—	—	—	97.0	~2.460	~6.3	—
$\text{CH}_2\text{OHCH}_2\text{NH}_3^{\text{b}}$	95.9	2.312	13.8	-6	0.1182	95.7	2.456	14.9	-60
Melaminium ²⁺	95.8	2.334	7.6°	-28	0.1140	95.6	2.468	7.5	-113
$\text{Me}_4\text{enH}_5^{2+}$	96.4	2.322	17.9°	-23	0.1130	95.7	2.451	17.1°	-134
$(\text{CH}_3)_2\text{CHNH}_3^{\ddagger}$	95.5	2.308	19.2°	-14	0.1125	95.1	2.446	18.3	-90
Piperazinium ²⁺	95.8	2.324	23.2	-13	0.1093	—	—	—	—
$(\text{CH}_3)_2\text{NH}_2^{\ddagger}$	95.6	2.326	23.6	~15	0.1018	—	—	—	-60
Piperidinium ⁺	95.5	2.288	29.6	26	0.1042	—	—	—	-9
4- $\phi\text{CH}_2\text{C}_8\text{H}_{11}\text{N}^{\dagger}$	95.3	2.311	28.7	30	0.0916	—	—	—	—
$\text{MeNH}_2\text{C}_2\text{H}_4\phi^{\dagger}$	95.1	2.339	46.1	70	—	—	—	—	—
Paraquat ²⁺	97.5	2.318	31.7	-19	0.111	—	—	—	-74

^a References therein; ^b The distortion in this salt yields a geometry closer to square pyramidal.

other geometrical parameters—e.g., bond lengths, non-bridging angles, semi-coordinate interactions, etc. This is borne out by extended Huckel calculation for the chloride salts (O'Brien *et al* 1986) in the spirit of the Hoffmann approach, where J_{AF} is proportional to $(\epsilon_1 - \epsilon_2)^2$. A comparison of the measured J/k values with the calculated $(\epsilon_1 - \epsilon_2)^2$ values in table 2 shows good correlation, even when the J/k vs σ correlation shows its largest scatter.

3. Magnetism of $\text{Cu}_3\text{X}_8^{2-}$ and $\text{Cu}_4\text{X}_{10}^{2-}$ oligomers

3.1 Structural properties

In addition to the dinuclear oligomers discussed in the previous section, we have prepared a large number of $n = 3$ (Grigereit *et al* 1986) and $n = 4$ oligomers (Rubenacker *et al* 1986; Halvorson *et al* 1986). These are characterized by the existence of pseudo-planar bridged structures, 1 and 2 (Rubenacker *et al* 1986; Halvorson *et al* 1986), with $\text{X} = \text{Cl}^-$ or Br^- and $\text{L} = \text{Cl}^-$, Br^- , or a neutral ligand. They are conveniently visualized as finite segments of the infinite chains present in

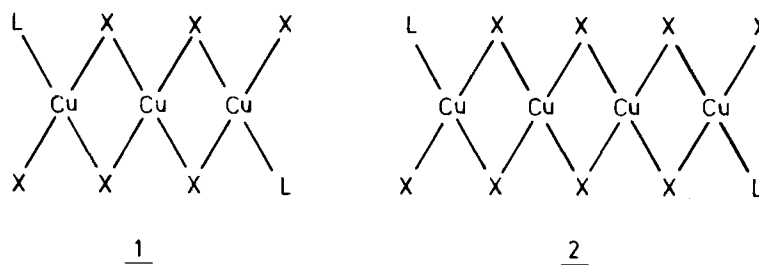


Chart 1.

the anhydrous CuX_2 salts. The $A_2Cu_nX_{2n+2}$ salts are synthesized by crystallization of the AX salt from aqueous and/or alcoholic solution with excess CuX_2 present. Within each oligomer, the copper ions have basically a square planar coordination geometry. The bridging $Cu-Cl-Cu$ angles range from 93° to 95° . Thus, an AFM exchange coupling is anticipated within the oligomers. As with the stacked dimers, the copper(II) ions within the oligomers complete their coordination sphere by forming one or two semi-coordinate bonds to halide ions in adjacent oligomers. The stacking patterns thus formed are shown in figure 3.

The magnetic behavior of the isolated copper(II) trinuclear species can be modeled by the nearest neighbour Heisenberg Hamiltonian

$$\mathcal{H} = -2J(\mathbf{S}_1 \cdot \mathbf{S}_2 + \mathbf{S}_2 \cdot \mathbf{S}_3), \quad (3)$$

which has energy levels $E_1 = 2J$ ($S = \frac{1}{2}$), $E_2 = 0$ ($S = \frac{1}{2}$), and $E_3 = -J$ ($S = 3/2$). For AFM coupling ($J < 0$), the E_1 level lies low in energy. The susceptibility of the system is given by

$$\chi_M = N_1\chi_{1/2} + N_2\chi_{1/2} + N_3\chi_{3/2} \quad (4)$$

where N_i is the population of the i th level and χ_s is the molecular (4) susceptibility of a state with spin S .

For the tetramers, the data were fit to a nearest neighbor Heisenberg Hamiltonian,

$$\mathcal{H} = -2J_1(\mathbf{S}_1 \cdot \mathbf{S}_2 + \mathbf{S}_3 \cdot \mathbf{S}_4) - 2J_2(\mathbf{S}_2 \cdot \mathbf{S}_3).$$

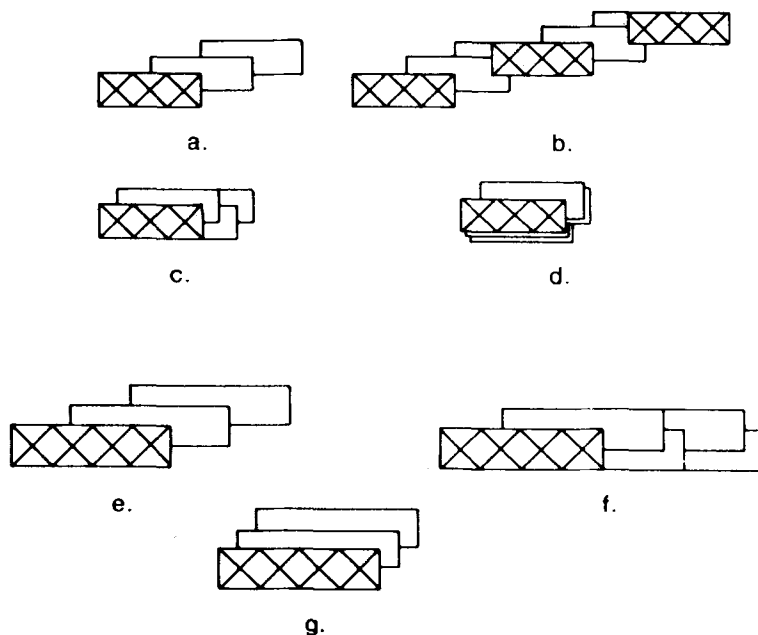


Figure 3. Stacking patterns for trimeric and tetrameric copper(II) halide oligomers.

where J_1 is the exchange constant between the outer pair of copper(II) ions and J_2 is the central exchange constant. This model has been solved exactly (Rubenacker *et al* 1986) and the magnetic susceptibility is given as

$$\begin{aligned} \chi = & (N_0 g^2 \mu \beta^2 / kT) [10 \exp(-E_1/kT) + 2 \exp(-E_2/kT) \\ & + 2 \exp(-E_3/kT) + 2 \exp(-E_4/kT)] \\ & \times (1 - x)/Z + x N_0 g^2 \mu \beta^2 / kT, \end{aligned} \quad (5)$$

where Z is the partition function, x is the fraction of tetrameric impurity, and the energy levels and spin degeneracies are

$$\begin{array}{ll} E_1 = -J_1 - (1/2)J_2, & S_1 = 2, \\ E_2 = J_1 - (1/2)J_2, & S_2 = 1, \\ E_3 = (1/2)J_2 + [J_1^2 + J_2^2]^{1/2}, & S_3 = 1, \\ E_4 = (1/2)J_2 - [J_1^2 + J_2^2]^{1/2}, & S_4 = 1, \\ E_5 = J_1 + (1/2)J_2 + [4J_1^2 - 2J_1J_2 + J_2^2]^{1/2}, & S_5 = 0, \\ E_6 = J_1 + (1/2)J_2 - [4J_1^2 - 2J_1J_2 + J_2^2]^{1/2}, & S_6 = 0. \end{array}$$

3.2 Trimeric systems

We will first examine the magnetic behavior of $\text{Cu}_3\text{Cl}_6(\text{CH}_3\text{CN})_2$, which illustrates the expected behavior of a simple trimer system. It forms stacks as in figure 3b. Figure 4a shows a plot of χ_M vs T for $\text{Cu}_3\text{Cl}_6(\text{CH}_3\text{CN})_2$, while figure 4b gives a plot of $\chi_M T$ vs T for the same salt. The gradual depopulation of the quartet state predicted by the Boltzman distribution now is evident in figure 4b where the $\chi_M T$ data shows a gradual decrease initially as T decreases, then a more rapid decrease near $T = 50$ K, and then a leveling out at the expected $S = \frac{1}{2}$ value at low temperature. In the χ_M data, χ_M increases steadily as T is lowered. The theory reproduces this behavior very accurately. However, qualitatively different behavior is seen for salts which stack as in figures 3c or 3d. As seen in figures 5a and 5b, the value of $\chi_M T$ for $(3\text{MAP})_2\text{Cu}_3\text{Cl}_8$ stays more level at high temperature and drops more rapidly than predicted by the simple theory (dashed line, figure 7b). The χ_M data also shows this in that χ_M reaches a plateau where it stays essentially constant over a wide temperature range. Inclusion of a J_{13} term in (3) cannot reproduce this behavior. In essence, we are seeing evidence of a cooperative (non-Boltzman-like) behavior with the quartet state staying populated longer than expected. Other salts studied with similar stacking patterns show this behavior to a greater or lesser extent.

A possible explanation of this phenomenon may be related to the phenomenon of spin frustration. In 3 below, we see several possible spin arrangements between adjacent trimers in one stack of the type illustrated in figure 3a with intertrimer exchange pathways J' indicated. In 3b, the interaction between two ground spin $\frac{1}{2}$ states are considered. If all J' have the same sign, then the spin at site 1' is frustrated, i.e., it gets conflicting spin alignment messages via J_{11}' and J_{21}' . The same is true for the spin at site 2'. In 3c, the interaction between spin $\frac{1}{2}$ and spin $\frac{3}{2}$ states is depicted. Again, spins 1' and 2' are frustrated. However, this is not the

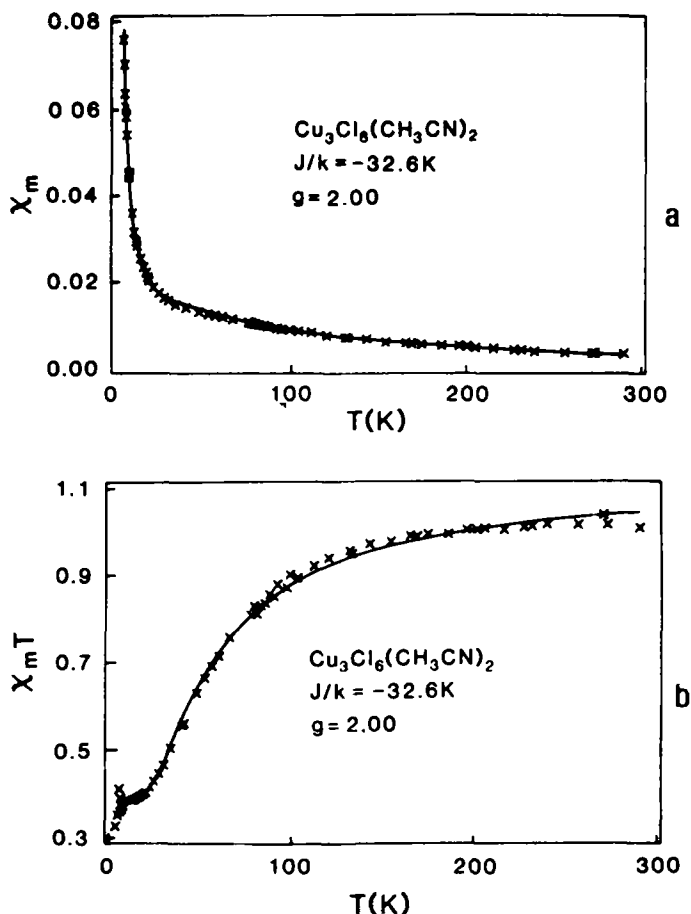


Figure 4. a. χ_M vs T for $Cu_3Cl_6(CH_3CN)_2$. b. $\chi_M T$ vs T for $Cu_3Cl_6(CH_3CN)_2$.

case for two adjacent spin $3/2$ states (3d) when J' is positive. Then the spin alignment information at sites $1'$ and $2'$ is consistent. Thus, it will cost less energy to form two adjacent $S = 3/2$ states than two isolated ones. That is, the population of the $3/2$ state stays larger than predicted by Boltzman statistics as long as it has an appreciable population. We can account for this in a phenomenological matter by applying a FM mean field correction to the quartet state (irrespective of the sign of J') as in (6),

$$\chi_M = N_1\chi_{1/2} + N_2\chi_{1/2} + N_3 [T/(T-\theta)] \chi_{3/2}. \quad (6)$$

This gives an excellent fit to the data, as given by the solid line in figure 5b.

The data for the salts studied are summarized in table 3. For the Cl salts, J/k ranges from $-20K$ to $-33K$. The AFM coupling in the Br salt studied is considerably larger ($-100K$), as observed in other AFM systems.

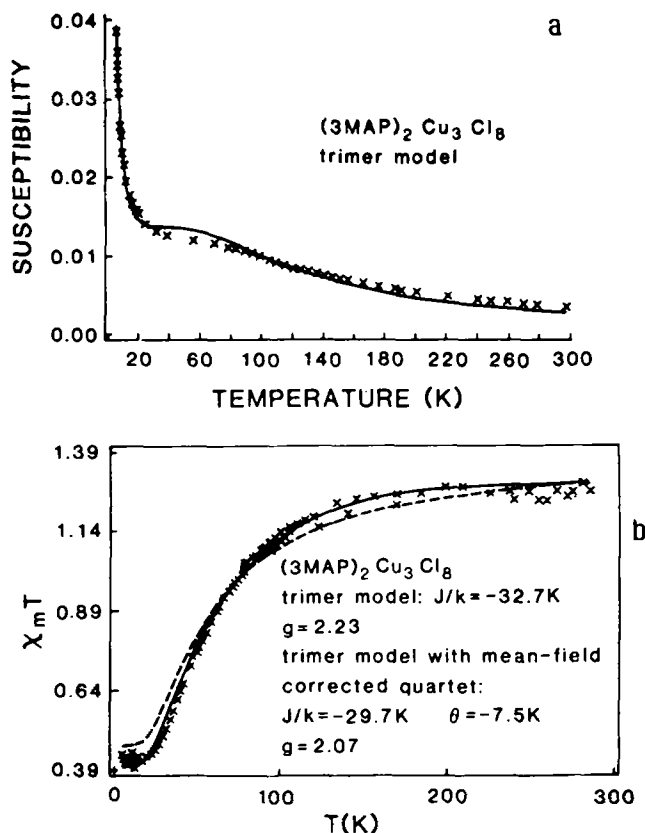


Figure 5. a. χ_M vs T for $(3\text{MAP})_2\text{Cu}_3\text{Cl}_8$. b. $\chi_M T$ vs T for $(3\text{MAP})_2\text{Cu}_3\text{Cl}_8$.

3.3 Tetrameric system

Three pseudo-planar $\text{Cu}_4\text{X}_{10}^{2-}$ systems have been studied, two chloride salts (Halvorson *et al* 1986) and one bromide salt (Rubenacker *et al* 1986). In each case, the central bridging angles ($\sim 93.5^\circ$) are smaller than the outer bridging angles ($\sim 94.5^\circ$). The magnetic data [figure 6 for $(\text{NMe}_4)_2\text{Cu}_4\text{Cl}_{10}$] is characteristic of antiferromagnetic coupling and exhibits the usual paramagnetic "impurity" tail. The data are very similar to that obtained from AFM dimers, and thus it is assumed that strong AFM coupling, J_1 , exists between the end pair of copper atoms and that weaker coupling, J_2 , exists between the central pair of copper atoms. Because of this strong AFM coupling between the end pairs, the spin system is essentially coupled at temperatures above which coupling between the central pairs becomes significant. This means that the data analysis is insensitive to the coupling between the central pairs. It is found that $J_1/k = -62\text{K}$ for $(4\text{MAP})_2\text{Cu}_4\text{Cl}_{10}$, $J_1/k = -64\text{K}$ for $(\text{NMe}_4)_2\text{Cu}_4\text{Cl}_{10}$, and $J_1/k = -180\text{K}$ for $(\text{Me}_3\text{NH})_2\text{Cu}_4\text{Br}_{10}$. The stronger AFM coupling for the Br system is again noted.

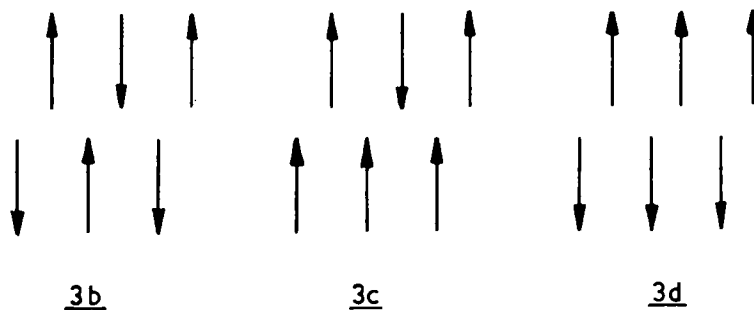
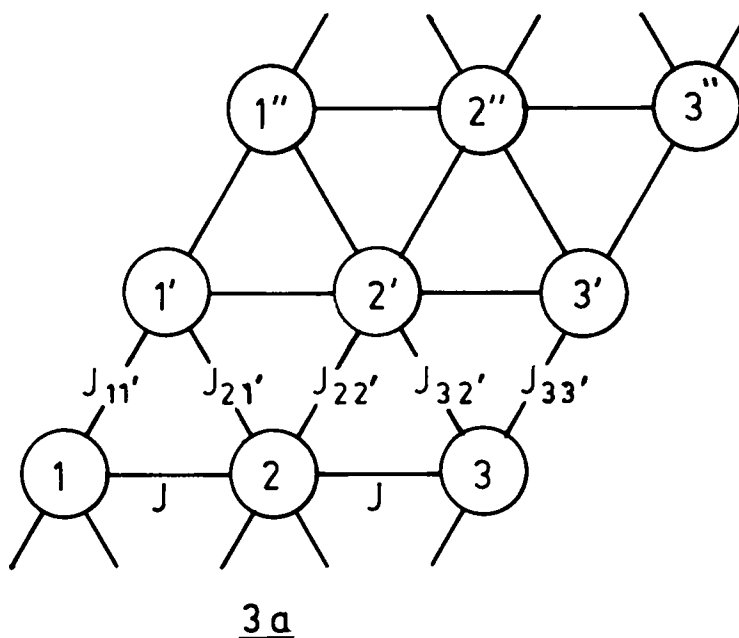


Chart 2.

Table 3. Magnetic parameters for pseudo-planar bibriged copper(II) chloride trimers.

Compound	J/k_a	theta	g
NMPZ	-29.4(3)	-1.7(2)	2.183(7)
NMPA	-19.4(1)	-4.9(2)	2.053(7)
3MAP	-29.7(3)	-7.5(3)	2.067(9)
CH ₃ CN	-32.6(5)	0	2.004(4)

4. Discussion

In examining the data for the summarized series of symmetrically bibriged copper(II) chloride and bromide salts, discussed above, it is worthwhile examining the role of the bridging ligand. For most ferromagnetic salts in the series, the

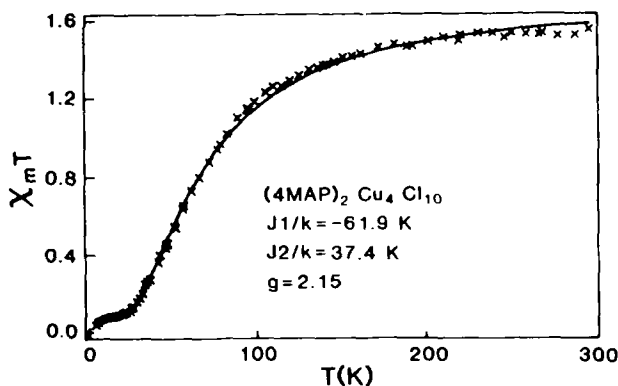


Figure 6. Plot of $\chi_M T$ vs T for $(4\text{MAP})_2\text{Cu}_4\text{Cl}_{10}$.

magnitude of J/k is approximately the same irrespective of the ligand. However, as the salts become antiferromagnetic, J/k decreases much more rapidly for the bromide salts than chloride salts. For those salts where structures are known for both the chloride and bromide analogs, little difference in the structures occur, other than those attributable to the larger ionic radius of the bromide ion. Thus, these trends cannot be accounted for by structural arguments. The cause can be readily seen, however, by examining the factors which affect the antiferromagnetic contribution to the exchange (Willett 1986). Hay *et al* (1978) argue that the value of $(\epsilon_1 - \epsilon_2)$ in (1) is inversely proportional to the difference in energies between the ligand orbitals and the magnetic orbital on the metal. This quantity may be estimated from the intense ligand-to-metal charge transfer transitions, which occur at the UV-visible borderline for the chloride salts ($\sim 25\text{--}30,000\text{ cm}^{-1}$) but are in the middle of the visible region for the bromide salts ($\sim 15\text{--}20,000\text{ cm}^{-1}$). Thus, it is expected that the antiferromagnetic contribution to the exchange, J_{AF} , will be 2–3 times larger for the bromide salts than for the chloride salts. This is in excellent agreement with the experimental trends, as can be seen in figure 7 where $J(\text{Cl})$ is plotted vs $J(\text{Br})$. A rough linear relationship is readily observed, with a slope of approximately $\frac{1}{2}$.

A comparison of the correlation of J/k values with oligomer size for pseudoplanar $\text{Cu}_n\text{X}_{2n}^{2-}$ anions (table 4) reveals some very interesting, but unexpected, trends. It is observed that J tends to become more negative, while ϕ decreases, as n increases. For planar bridged $\text{Cu}(\text{II})$ systems, it is well established that as the bridging Cu-X-Cu angle increases, J becomes more antiferromagnetic (Fletcher *et al* 1983; Willett 1986). From table 4, it is seen that the compound with the smallest angle, CuBr_2 , $\phi = 92.1^\circ$, has one of the strongest antiferromagnetic coupling constants, $J/k = -165\text{ K}$. Thus, additional factors must be operative to account for these trends. One parameter of significance is certainly the Cu-X bond lengths in the bridge, since the delocalization of the magnetic electron out onto the ligands decreases as the Cu-X distance increases. Thus, shorter distances should lead to stronger antiferromagnetic coupling due to increased overlap. The bridging Cu-X bond lengths in dimeric species are particularly long, since the *trans* effect of the shorter terminal Cu-X bonds causes *all* bridging bonds to be elongated. In

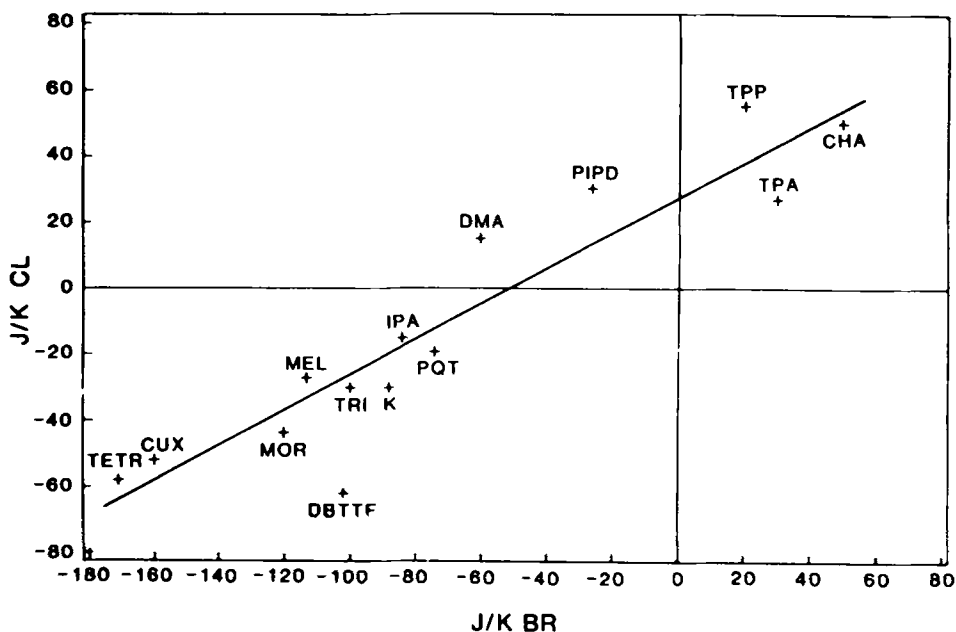


Figure 7. Plot of $J(\text{Cl})$ vs $J(\text{Br})$ for bridged copper(II) halide systems. (TETR = $\text{Cu}_4\text{X}_{10}^{2-}$ tetramers, $\text{CuX} = \text{CuX}_2$, MOR = morpholinium, MEL = melaminium, TRI = $\text{Cu}_3\text{X}_6^{2-}$ trimers, DBTTF = dibenzatetrafulvalenium, K = potassium, IPA = isopropylammonium, PQT = paraquat, DMA = dimethylammonium, TTP = tetraphenylphosphonium, TPA = tetraphenylarsonium, CHA = cyclohexylammonium.)

Table 4. J/k values for $\text{Cu}_n\text{X}_{2n+2}^{2-}$ oligomers.

n	X = Cl^-		X = Br^-	
	ϕ	J/k	ϕ	J/k
2	95.6°	-28 K	$\sim 96^\circ$	-95 K
3	94°	-30 K	94°	-100 K
4	94.5°	-60 K	94.8°	-180 K
∞	—	-55 K	92.1°	-165 K

trimers and tetramers, only half of the bridging Cu–X distances are elongated. Thus, an increase in antiferromagnetic contribution is expected for $n > 2$. Other effects must account for the difference between the exchange coupling for the trimers and the terminal bridges in the tetramer, as well as for the infinite chains. Possible effects include the unusually large terminal X–Cu–X angle, variations in the semi-coordinate Cu...X distances, and small deviations from non-planarity. Theoretical calculations to explore these factors are planned.

Acknowledgement

The support of NSF grant DMR-8219430 is gratefully acknowledged.

References

- Bencini A and Gatteschi D 1978 *Inorg. Chim. Acta* **31** 11
- Bencini A, Gatteschi D and Zanchini C 1985 *Inorg. Chem.* **24** 700
- Chow C, Willett R D and Gerstein B C 1975 *Inorg. Chem.* **14** 205
- Fletcher R, Hansen J J, Livermore J and Willett R D 1983 *Inorg. Chem.* **20** 330
- Geiser U and Willett R D 1984 *Croat. Chem. Acta* **57** 737
- Geiser U, Willett R D, Lindbeck M J and Emerson K 1986 *J. Am. Chem. Soc.* **108** 1173
- Grigereit T, Ramakrishna B L, Place H, Willett R D, Pellacani G C, Manfredini T, Menabue L, Bonamartini-Corradi A and Battaglia L P 1987 *Inorg. Chem.* (submitted)
- Hall J W, Marsh W E, Welles R R and Hatfield W E 1981 *Inorg. Chem.* **20** 1033
- Halvorson K E, Grigereit T and Willett R D 1987 *Inorg. Chem.* (accepted)
- Hatfield W E 1985 in *Magneto-structural correlation in exchange-coupled systems NATO ASI series* (eds) R D Willett, O Kahn and D Gatteschi (New York: Plenum Press)
- Hay P J, Thiebault S C and Hoffmann R 1978 *J. Am. Chem. Soc.* **97** 4884
- Honda M, Katayama C, Tanaka J and Tanaka M 1985 *Acta Crystallogr.* **C41** 187, 688
- Kahn O and Briat B 1976 *J. Chem. Soc. Faraday Trans II* **72** 268
- Kahn O and Charlot M F 1980 *Nuovo. J. Chim.* **4** 576
- O'Brien S, Gaura R M, Landee C P, Ramakrishna B L and Willett R D 1987 *Inorg. Chem.* (accepted)
- Pellacani G C, Manfredini T, Scott B, Geiser U and Willett R D 1987 (in preparation)
- Rubenacker G V, Drumheller J E, Emerson K and Willett R D 1986 *J. Magn. & Magn. Mater.* **54-57** 1483
- Scott B and Willett R D 1987 *J. Appl. Phys.* (accepted)
- Smith D W 1976 *Coord. Chem. Rev.* **21** 93
- Willett R D 1985 in *Magneto-structural correlations in exchange-coupled systems, NATO ASI series* (eds) R D Willett, D Gatteschi and O Kahn (New York: Plenum Press) p. 269
- Willett R D and Geiser U 1984 *Acta Chem. Croat.* **57** 751
- Willett R D 1986 *Inorg. Chem.* **25** 1918, and references therein